Variational and diffusion quantum Monte Carlo calculations at nonzero wave vectors: Theory and application to diamond-structure germanium

G. Rajagopal and R. J. Needs
Cavendish Laboratory, Madingley Road, Cambridge CB3 0HE, United Kingdom

A. James
The Blackett Laboratory, Imperial College of Science, Technology and Medicine, Prince Consort Road, London SW7 2BZ, United Kingdom

S. D. Kenny
Cavendish Laboratory, Madingley Road, Cambridge CB3 0HE, United Kingdom

W. M. C. Foulkes
The Blackett Laboratory, Imperial College of Science, Technology and Medicine, Prince Consort Road, London SW7 2BZ, United Kingdom

(Received 4 October 1994)

A variational and diffusion quantum Monte Carlo study of germanium in the diamond structure is reported, in which local pseudopotentials are used to represent the ion cores. We calculate the energy of the free atom and the energy of the solid as a function of volume. The calculations for the solid are performed using a supercell method. We analyze the translational symmetry of the supercell Hamiltonian and show that the eigenstates can be labeled by two wave vectors, $\mathbf{k}_s$ and $\mathbf{k}_p$. The wavevector $\mathbf{k}_s$ arises from the invariance of the Hamiltonian under the translation of any one-electron coordinate by a supercell translation vector, while the wave vector $\mathbf{k}_p$, which is the crystal momentum of the wave function, arises from the invariance under the simultaneous translation of all electron coordinates by a translation vector of the crystal lattice. Our solid calculations are performed using wave functions with nonzero supercell wave vectors $\mathbf{k}_s$, which gives better convergence with the size of supercell than previous zero-wave-vector calculations. The relationship of this method to the special k-points techniques commonly used in band-structure calculations is discussed.

I. INTRODUCTION

Quantum Monte Carlo (QMC) methods offer the possibility of performing highly accurate calculations on many-body electronic systems. In variational quantum Monte Carlo (VMC) (Ref. 1), the energy is calculated as the expectation value of the Hamiltonian with an approximate trial wave function, and the required multidimensional integrals are evaluated using a Monte Carlo method. The accuracy of a VMC calculation is ultimately limited by the quality of the many-body wave function used, which may contain a number of variable parameters. In the diffusion quantum Monte Carlo (DMC) method,[2] a distribution is generated via propagation of the imaginary-time Schrödinger equation from which, in principle, exact energies can be calculated. This method makes use of importance sampling, in which the guiding wave function is used to bias the sampling towards regions where the wave function is large, thereby reducing the variance of the estimate of the energy. To make the calculations tractable the so-called fixed-node approximation[3,4] is normally used, in which the nodal surface of the wave function is constrained to be equal to that of an approximate guiding wave function. The fixed-node approximation, which often leads to very satisfactory results, overcomes the so-called sign problem, which plagues most fermion QMC methods. A second approximation is normally made in DMC calculations, the so-called short-time approximation, but the effect of this can usually be made very small.

Variational quantum Monte Carlo and DMC methods of the type discussed here have been widely used in studies of electronic systems with small numbers of particles, such as atoms and molecules,[3] and jellium spheres.[5] Applications to solids have used periodic boundary conditions to reduce the number of particles to a manageable size of up to a few hundred. The number of applications to solids is still quite small; we note in particular studies of the homogeneous electron gas (jellium),[4] a jellium surface,[6] phases of solid hydrogen,[7] and pseudopotential studies of solids composed of heavier atoms such as carbon,[8,9] silicon,[9,10] germanium,[11] and nitrogen.[12]

Recently, we introduced a method for performing VMC and DMC calculations for periodic solids with wave functions having nonzero wave vectors.[11] Performing calculations at non-zero wave vectors allows the adoption of a set of ideas familiar from band structure theory known as special k-points methods.[13–15] In band-structure calculations these methods are used to perform accurate Brillouin zone (BZ) integrations for insulating solids using only a small number of k-points, which corresponds to considering a system with a small number of particles and periodic boundary conditions. We have shown that these ideas can be applied to VMC and DMC calculations,[11] giving excellent results for small system sizes, so that the finite-size effects are significantly reduced. The purpose of this paper is twofold: first to describe in detail the theory of performing VMC and DMC calculations with non-zero wave vectors, and second to report results for the energy of diamond-structure germanium as a function of volume.

II. TRANSLATIONAL SYMMETRIES OF THE SUPERCELL HAMILTONIAN

We start with a careful study of the translational symmetries of the Hamiltonian, $\hat{H}$, used in supercell many-body calculations for electronic systems. $\hat{H}$ can be written in the form[16]

$$\hat{H} = -\frac{1}{2}\sum_{i=1}^{N}\nabla_i^2 + \sum_{\mathbf{R}_s}\sum_{i>j}^{N}\frac{1}{|\mathbf{r}_i - \mathbf{r}_j - \mathbf{R}_s|} + \sum_{i=1}^{N}V(\mathbf{r}_i), \tag{1}$$

where $\{\mathbf{R}_s\}$ is the set of translation vectors of the supercell lattice, the potential $V(\mathbf{r})$ has the periodicity of $\{\mathbf{R}_s\}$, and N is the number of electrons in the supercell. In supercell many-body calculations one is often interested in the case where the primitive translation vectors of the supercell lattice are integer multiples of the primitive translation vectors of an underlying crystal lattice. These integer multiples are denoted by n_i and we refer to a $n_1 \times n_2 \times n_3$ supercell. It follows that $V(\mathbf{r})$ has the periodicity of the set, $\{\mathbf{R}_p\}$ of translation vectors of the underlying crystal lattice, of which $\{\mathbf{R}_s\}$ is a subset.

The Hamiltonian $\hat{H}$ has two different translational symmetries:

(i) $\hat{H}$ is invariant under the translation of any electron coordinate by a vector in $\{\mathbf{R}_s\}$.

(ii) $\hat{H}$ is invariant under the simultaneous translation of all electron coordinates by a vector in $\{\mathbf{R}_p\}$.

Symmetry (ii) holds for the Hamiltonian of the truly infinite system, but symmetry (i) arises from the use of the supercell method. We will now demonstrate that each of these symmetries results in a Bloch type condition, and that the Bloch eigenfunctions of $\hat{H}$ can be labeled by two separate wave vectors, denoted by $\mathbf{k}_s$ and $\mathbf{k}_p$.

Symmetry (i) implies that the wave function can only change by a phase factor when any single electron is translated by a supercell lattice vector. The indistinguishability of the electrons then implies that the phase factor must be the same no matter which electron is moved. This may be demonstrated by applying Bloch's theorem separately to the first and second arguments of the wave function, assuming for the moment that the corresponding $\mathbf{k}$-vectors are different:

$$\Psi(\mathbf{r}_1, \mathbf{r}_2, ...) = e^{-i\mathbf{k}_1\cdot\mathbf{R}_s}\Psi(\mathbf{r}_1 + \mathbf{R}_s, \mathbf{r}_2, ...), \tag{2}$$

$$\Psi(\mathbf{r}_1, \mathbf{r}_2, ...) = e^{-i\mathbf{k}_2\cdot\mathbf{R}_s}\Psi(\mathbf{r}_1, \mathbf{r}_2 + \mathbf{R}_s, ...). \tag{3}$$

Applying the permutation symmetry to Eq. (2) gives

$$\Psi(\mathbf{r}_1, \mathbf{r}_2, ...) = -e^{-i\mathbf{k}_1\cdot\mathbf{R}_s}\Psi(\mathbf{r}_2, \mathbf{r}_1 + \mathbf{R}_s, ...). \tag{4}$$

Translating the second argument by $-\mathbf{R}_s$ gives

$$\Psi(\mathbf{r}_1, \mathbf{r}_2, ...) = -e^{-i(\mathbf{k}_1-\mathbf{k}_2)\cdot\mathbf{R}_s}\Psi(\mathbf{r}_2, \mathbf{r}_1, ...), \tag{5}$$

and using the permutation symmetry once more yields

$$\Psi(\mathbf{r}_1, \mathbf{r}_2, ...) = e^{-i(\mathbf{k}_1-\mathbf{k}_2)\cdot\mathbf{R}_s}\Psi(\mathbf{r}_1, \mathbf{r}_2, ...). \tag{6}$$

It, therefore, follows that

$$\mathbf{k}_1 - \mathbf{k}_2 \in \{\mathbf{G}_s\}, \tag{7}$$

where $\{\mathbf{G}_s\}$ is the set of vectors reciprocal to $\{\mathbf{R}_s\}$. The phase factor $\exp(-i\mathbf{k}_1\cdot\mathbf{R}_s)$ is unchanged when a vector in $\{\mathbf{G}_s\}$ is added to $\mathbf{k}_1$ and, therefore, $\mathbf{k}_1$ may be reduced into the first BZ of the supercell reciprocal lattice. Consequently, we can choose $\mathbf{k}_1 = \mathbf{k}_2 = \mathbf{k}_s$, without loss of generality, and Ψ can be written in the form

$$\Psi_{\mathbf{k}_s}(\{\mathbf{r}_i\}) = U_{\mathbf{k}_s}(\{\mathbf{r}_i\})\ \exp\left(i\mathbf{k}_s\cdot\sum_{i=1}^{N}\mathbf{r}_i\right), \tag{8}$$

where $U_{\mathbf{k}_s}$ is invariant under the translation of any electron coordinate by a vector in $\{\mathbf{R}_s\}$, and is antisymmetric under particle exchange. [We have omitted the band index in Eq. (8) and elsewhere, as we will be concerned only with the lowest band.]

We now consider translational symmetry (ii) of $\hat{H}$. The operators, generating the simultaneous translation of all electron coordinates by a vector in $\{\mathbf{R}_p\}$ form the same symmetry group as the standard one-electron translation operators, which occur in the proof of Bloch's theorem found in many textbooks. The irreducible representations may be labeled by a single wave vector and the eigenfunctions of Eq. (1) transform according to

$$\Psi(\{\mathbf{r}_i + \mathbf{R}_p\}) = e^{i\mathbf{k}_p\cdot\mathbf{R}_p}\ \Psi(\{\mathbf{r}_i\}), \tag{9}$$

where the wave vector $\mathbf{k}_p$ is the crystal momentum of the wave function, and $\mathbf{k}_p$ can be reduced into the first BZ of the lattice reciprocal to $\{\mathbf{R}_p\}$, which we refer to as the primitive BZ. It follows that the eigenfunctions of Eq. (1) can also be written in the form

$$\Psi_{\mathbf{k}_p}(\{\mathbf{r}_i\}) = W_{\mathbf{k}_p}(\{\mathbf{r}_i\})\ \exp\left(i\mathbf{k}_p\cdot\frac{1}{N}\sum_{i=1}^{N}\mathbf{r}_i\right), \tag{10}$$

where $W_{\mathbf{k}_p}$ is invariant under the simultaneous translation of all electron coordinates by a vector in $\{\mathbf{R}_p\}$, and is antisymmetric under particle exchange.

The operators which generate the translation of all electrons by a vector in $\{\mathbf{R}_p\}$ and the operators which generate the translation of an electron by a vector in $\{\mathbf{R}_s\}$ commute with one another. It, therefore, follows that the eigenfunctions of Eq. (1) can be chosen to satisfy Eqs. (8) and (10) simultaneously, whereupon $U_{\mathbf{k}_s}$ and $W_{\mathbf{k}_p}$ differ only by a phase factor, which depends on the positions of the electrons. Because the set $\{\mathbf{R}_s\}$ is a subset of $\{\mathbf{R}_p\}$ there is a relationship between $\mathbf{k}_s$ and $\mathbf{k}_p$. If we write the wave function in the form of Eq. (10), and translate all electron coordinates by a supercell translation vector, $\mathbf{R}_s$, then we obtain the same relation as Eq. (9), but with $\mathbf{R}_p$ replaced by $\mathbf{R}_s$. Performing the same translations on the wave function of the form of Eq. (8) gives

$$\Psi(\{\mathbf{r}_i + \mathbf{R}_s\}) = e^{i\mathbf{k}_s\cdot N\mathbf{R}_s}\ \Psi(\{\mathbf{r}_i\}). \tag{11}$$

These two forms for $\Psi(\{\mathbf{r}_i+\mathbf{R}_s\})$ must be equal, and, therefore,

$$N\mathbf{k}_s-\mathbf{k}_p\in\{\mathbf{G}_s\}. \tag{12}$$

We emphasize that the simple relation $N\mathbf{k}_s=\mathbf{k}_p$ is only one of the possible ways to satisfy Eq. (12), and indeed most of the numerical results presented in this paper are for wave functions with $N\mathbf{k}_s\neq\mathbf{k}_p$. A complete description of the translational symmetry of the wavefunction is given by specifying both $\mathbf{k}_s$ and $\mathbf{k}_p$, and therefore we write $\Psi_{\mathbf{k}_s,\mathbf{k}_p}$.

In the limit of an infinite-sized supercell, the value of $\mathbf{k}_s$ must tend to zero for all wave functions of the form of Eq. (8). However, the ground state of a finite-sized supercell need not have $\mathbf{k}_s=0$ or $\mathbf{k}_p=0$. We have constructed an explicit example to illustrate this, consisting of a system of noninteracting electrons in a fixed periodic local potential, so that the ground state wave function is a single determinant, and the total energy is the sum of occupied band energies. The potential was obtained from a local-density approximation (LDA) calculation for diamond-structure germanium. We considered the smallest possible supercell, which is just the primitive unit cell, into which were placed six electrons, three spin-up, and three spin-down (not the eight electrons per unit cell of real germanium). In order to form a state with a definite $\mathbf{k}_s$, the one-electron orbitals must be chosen from a single k-point in the supercell BZ, which is the same as the primitive BZ in this case. The set of $\mathbf{k}_s$ values consistent with $\mathbf{k}_p=0$ forms a $6\times6\times6$ mesh within the primitive BZ centered at $\mathbf{k}=0$, and the lowest total band energy at a point on this mesh was obtained at $\mathbf{k}=(2/3,2/3,0)2\pi/a_0$ in Cartesian coordinates, where a_0 is the cubic lattice constant. However, k-points neighboring this point (but not on the mesh) gave lower total band energies, and, therefore, the ground state of this supercell cannot have $\mathbf{k}_p=0$ or $\mathbf{k}_s=0$. [For a local potential it is straightforward to show that the lowest energy orbital must have $\mathbf{k}=0$, so that for the special case of one electron in the supercell (or two electrons of opposite spin) the ground state must have $\mathbf{k}_p=0$ and $\mathbf{k}_s=0$.]

To conclude this section, we mention other symmetries of the functions $U_{\mathbf{k}_s}$ and $W_{\mathbf{k}_p}$. Time reversal symmetry implies that $U_{\mathbf{k}_s}(\{\mathbf{r}_i\})=U^*_{-\mathbf{k}_s}(\{\mathbf{r}_i\})$, and if, in addition, the potential $V(\mathbf{r})$ has inversion symmetry, then we can choose $U_{-\mathbf{k}_s}(\{\mathbf{r}_i\})=U_{\mathbf{k}_s}(\{-\mathbf{r}_i\})$. However, for an arbitrary wave vector, $\mathbf{k}_s$, the supercell periodic function $U_{\mathbf{k}_s}$ is complex, and cannot be chosen to be real unless $\mathbf{k}_s=0$. Of course $U_{\mathbf{k}_s}$ may satisfy other symmetry relations associated with the crystal symmetry of the potential $V(\mathbf{r})$. The function $W_{\mathbf{k}_p}$ satisfies similar relations.

III. TRIAL/GUIDING WAVE FUNCTIONS FOR VMC AND DMC CALCULATIONS

Typically the approximate wave function used in VMC calculations and the guiding wave function used in DMC calculations for solids is chosen to be of the Slater-Jastrow-Bijl form:

$$\Phi_{\mathbf{k}_s,\mathbf{k}_p}=\exp\Bigg[-\sum_{\mathbf{R}_s}\sum_{i>j}^{N}u(|\mathbf{r}_i-\mathbf{r}_j-\mathbf{R}_s|)+\sum_{i=1}^{N}\chi(\mathbf{r}_i)\Bigg]D_{\mathbf{k}_s,\mathbf{k}_p}, \tag{13}$$

where the function $u(r)$ correlates the electrons in pairs, $\chi(\mathbf{r})$ is a one-body function, and $D_{\mathbf{k}_s,\mathbf{k}_p}$ is a determinant of single-particle orbitals. $\chi(\mathbf{r})$ is chosen to have the periodicity of $\{\mathbf{R}_p\}$ (and any other symmetries of the crystal) and the u term is invariant under translations of all electron coordinates by any constant vector as well as under translations of a single-electron coordinate by vectors in $\{\mathbf{R}_s\}$.

It is certainly not necessary to use Bloch wave functions with well defined values of $\mathbf{k}_s$ and $\mathbf{k}_p$ in QMC calculations, and for some purposes it might be advantageous to use linear combinations of degenerate Bloch wave functions. For example, one can always form real wave functions from a linear combination of Bloch wave functions with $\pm\mathbf{k}_s$ or $\pm\mathbf{k}_p$. However, the Bloch wave functions are convenient for our purposes and are used throughout this paper. To form a wave function of the form of Eq. (13), the values of the wave vectors $\mathbf{k}_s$ and $\mathbf{k}_p$ are determined by the wave vectors of the states which enter the determinant, which we denote as $\mathbf{k}_i$, where each $\mathbf{k}_i$ lies within the primitive BZ. In order to form a determinant, which has a definite $\mathbf{k}_s$, it is necessary that the one-electron states all have the same wave vector when reduced into the supercell BZ, which corresponds to a regular mesh or lattice of wave vectors in the primitive BZ. The translation vectors of this mesh are the set $\{\mathbf{G}_s\}$, the offset of the mesh from the origin gives the value of $\mathbf{k}_s$, and the wave vector $\mathbf{k}_p$ is equal to $\sum_i\mathbf{k}_i$. In our work the single-particle orbitals are obtained from self-consistent LDA calculations, which will be discussed in more detail later in this paper.

For the u function, we use the common form[4]

$$u_{\sigma_i,\sigma_j}(r_{ij})=\frac{A}{r_{ij}}\left[1-\exp\left(-\frac{r_{ij}}{F_{\sigma_i,\sigma_j}}\right)\right], \tag{14}$$

where r_{ij} is the distance between electrons i and j, σ_i denotes the spin of electron i, and A and F_{σ_i,σ_j} are constants. We impose the cusp conditions,[17] which constrain the form of the wave function as $r_{ij}\to0$, and lead to $F_{\sigma_i,\sigma_j}=\sqrt{(2A)}$ for parallel spins and $F_{\sigma_i,\sigma_j}=\sqrt{A}$ for antiparallel spins. The only free parameter in u is then A, which we set equal to $1/\sqrt{(4\pi N/\Omega)}$, where N/Ω is the number of electrons per unit volume. This form for A is motivated by previous work on the homogeneous electron gas, which showed that at large electron separations u should have a $1/r_{ij}$ dependence with a coefficient of $1/\omega_p$, where ω_p is the plasma energy.[4,18] This dependence of u on the plasma energy has been used with success in previous calculations on the homogeneous electron gas,[4] and on carbon[8,9] and silicon.[9,10]

The determinant of LDA orbitals generally gives a good description of the charge density. However, the addition of the correlation function, u, in Eq. (13), keeps

the electrons away from each other and produces a strong and unphysical smoothing of the charge density. The single-body χ function allows the electronic charge density to be altered to counteract this smoothing effect. We have used the prescription due to Fahy *et al.*[8,9] for obtaining a χ function, which returns the charge density towards the LDA form. In this prescription χ is given by

$$\chi(\mathbf{r}) = \frac{1}{2} \ln\left[\frac{\rho_{\mathrm{LDA}}(\mathbf{r})}{\rho_{u,\chi=0}(\mathbf{r})}\right], \tag{15}$$

where ρ_{LDA} is the LDA charge density and $\rho_{u,\chi=0}$ is the charge density obtained from a VMC calculation with a wave function of the form of Eq. (13), but with $\chi(\mathbf{r}) = 0$.

IV. SPECIAL k-POINTS METHODS FOR SUPERCELL MANY-BODY CALCULATIONS

Having understood that the eigenfunctions of the Hamiltonian of Eq. (1) can be labeled by the two wave vectors, $\mathbf{k}_s$ and $\mathbf{k}_p$, it is natural to ask the question "what values of $\mathbf{k}_s$ and $\mathbf{k}_p$ should be chosen to represent a particular physical situation?" If one is interested in excitation energies then the quantum number of interest is $\mathbf{k}_p$, but to obtain wave functions with different values of $\mathbf{k}_p$, it may be necessary to use wave functions with $\mathbf{k}_s \neq 0$, because $\mathbf{k}_s$ and $\mathbf{k}_p$ are linked via Eq. (12). We note a recent DMC study of solid nitrogen[12] in which a wave function with $\mathbf{k}_s = 0$ but $\mathbf{k}_p \neq 0$ was used to represent an excited state. We will deal with excitation energies elsewhere, and here we concentrate on the ground state properties, so that the question we address is "for a given size of supercell, what values of $\mathbf{k}_s$ and $\mathbf{k}_p$ should be chosen to represent most accurately the ground state of the infinite system?" The earlier calculations of Refs. 7–10 used wave functions with $\mathbf{k}_s = \mathbf{k}_p = 0$ for this purpose; however, the problem of choosing the finite system which best represents the infinite system has already been addressed within the context of band-structure calculations and, after rephrasing in our language, the conclusion is that one should certainly not use $\mathbf{k}_s = 0$, and should sometimes choose $\mathbf{k}_p \neq 0$ as well.

The method of special k points in band-structure theory is a technique for performing BZ integrations, using only a small number of k–points.[13–15] This method gives excellent results when integrating over full bands, but poorer results for partially occupied bands, and, therefore, the method is used mostly for insulating systems. The integration over the BZ is analogous to the integrals over configuration space performed in QMC calculations. In the original special k-points scheme of Baldereschi[13] a single k point in the BZ was selected such that the value at this point of, for example, the band-structure energy, gives the best estimate of the integral over the entire BZ. Subsequently multipoint schemes were introduced to obtain more accurate results, of which the Monkhorst-Pack (MP) scheme[14] has been the most widely used in band-structure calculations. The MP scheme consists of choosing a lattice or mesh of k points, whose translation vectors are defined by dividing each of the reciprocal-space translation vectors of the primitive cell, $\mathbf{b}_i$, by an integer n_i. In the original paper,[14] the offset of this mesh from the origin was fixed, but this condition was later relaxed.[15] It should be clear that, in the language of many-body supercell calculations, a determinant of single-particle orbitals, whose k vectors lie on a MP-type mesh, forms a wave function for an $n_1 \times n_2 \times n_3$ supercell with a definite value of $\mathbf{k}_s$, equal to the offset of the MP mesh from the origin.

The original analysis of Baldereschi[13] can be applied to the supercell rather than the primitive cell, to show that the best offset of the mesh is the Baldereschi mean value point of the supercell BZ. This often leads to a wave function with $\mathbf{k}_s \neq 0$ and $\mathbf{k}_p \neq 0$. Unfortunately, this choice is not always convenient because for some lattices (for example the fcc lattice used in our studies) the corresponding mesh of k points does not have inversion symmetry and therefore a determinant formed from these orbitals must be complex. Instead of choosing the Baldereschi point of the supercell BZ, we recommend the grid defined by offsetting the basic mesh from the origin by $\mathbf{G}_s/2$, where $\mathbf{G}_s$ is a supercell-reciprocal-lattice vector. This mesh always has inversion symmetry, and therefore, for a closed shell configuration, it is possible to form linear combinations of the orbitals which are real, from which a real determinant can be constructed.

It is important to realize that a determinant having a definite value of $\mathbf{k}_s \neq 0$ will not in general have the full symmetry of the lattice. The crystal symmetry is retrieved in the limit of a large supercell (i.e., large n_i). This symmetry breaking is not important for the total energy, but it may have undesirable effects on other quantities; for example the electronic charge density will not have the full crystal symmetry. The simplest way of dealing with this problem within QMC calculations is to symmetrize the charge density (or other quantity) after the calculation has been performed. Within LDA calculations a different approach is often adopted, in which the self-consistent calculation is performed on a symmetrized set of k points. This strategy normally results in an inferior value of the total energy because the theorems which underlie the success of the MP scheme do not apply. Even more serious problems arise if one tries to adopt this strategy within QMC calculations. The symmetrized mesh of k points may provide more linearly independent one-electron states than there are electrons in the supercell, and, therefore, a multideterminant wave function is required, which adds to the cost of the calculation. Moreover the resulting wave function may not have a definite value of $\mathbf{k}_s$, which means that the integrals over configuration space may need to be performed over a larger volume (see later).

The theory of why special k-points methods work well in band-structure-type calculations is well established, and we refer the reader to Refs. 13–15 for a detailed discussion. In crude terms, the bands have turning points at the center and edges of the primitive BZ, and, therefore, the best place to sample the BZ to get a good estimate of the mean band energy is roughly halfway between the zone center and the zone edge. We remark that LDA cal-

culations, which are essentially of band-structure type, normally give good results for solids, and indeed density-functional theory is in principle an exact theory of interacting electron systems cast as a band-structure method. It, therefore, seems natural that the basic ideas of special k-points methods should be transferable to QMC calculations. This justification is not phrased in the language of QMC calculations and so is not wholly satisfactory; but the successes reported in this paper and our previous paper[11] provide plenty of supporting evidence.

The purpose of the special k-points method is to obtain results for small supercell sizes, which accurately reflect the results which would be obtained for very large supercells. In QMC calculations for solids, it is normal to apply finite-size corrections, which are often calculated within the LDA. For the example studied in this paper of diamond-structure germanium these corrections work well, and the corrected QMC results are quite similar, whether or not the special k-points method is used. However, the most important applications of QMC will be to systems where the LDA works poorly. In such cases, the LDA finite-size corrections are unlikely to cancel the QMC finite-size errors accurately, and the special k-points method will be particularly useful.

V. SPECIAL CONSIDERATIONS FOR QMC CALCULATIONS

In VMC calculations the energy, E_{VMC}, is evaluated as

$$E_{\mathrm{VMC}} = \frac{\int (\Phi^*_{\mathbf{k}_s,\mathbf{k}_p}\Phi_{\mathbf{k}_s,\mathbf{k}_p})(\Phi^{-1}_{\mathbf{k}_s,\mathbf{k}_p}\hat{H}\Phi_{\mathbf{k}_s,\mathbf{k}_p})}{\int (\Phi^*_{\mathbf{k}_s,\mathbf{k}_p}\Phi_{\mathbf{k}_s,\mathbf{k}_p})} , \qquad (16)$$

where $\Phi_{\mathbf{k}_s,\mathbf{k}_p}$ is the approximate wave function, $(\Phi^*_{\mathbf{k}_s,\mathbf{k}_p}\Phi_{\mathbf{k}_s,\mathbf{k}_p})$ is a probability distribution, which is real and positive, and $(\Phi^{-1}_{\mathbf{k}_s,\mathbf{k}_p}\hat{H}\Phi_{\mathbf{k}_s,\mathbf{k}_p})$ is the local energy. The probability distribution is generated in a pointwise fashion, using a random walk procedure such as the Metropolis algorithm, and the local energy is accumulated (after a period of equilibration) along the walk. For general $\mathbf{k}_s$ and $\mathbf{k}_p$ vectors the local energy is complex at points along the walk, but in the limit of exact sampling the imaginary parts cancel from Eq. (16). The integrals in Eq. (16) are over all of configuration space, but by using the translational symmetry of $\Phi_{\mathbf{k}_s,\mathbf{k}_p}$ and $\hat{H}$, we can restrict the region over which the integrals need be evaluated. If an electron coordinate is translated by a vector in the set $\{\mathbf{R}_s\}$, then the wave function $\Phi_{\mathbf{k}_s,\mathbf{k}_p}$ is multiplied by a phase factor $e^{i\mathbf{k}_s\cdot\mathbf{R}_s}$, which leaves both the probability distribution and the local energy unaltered. It follows that the integrals in Eq. (16) need be performed only over a single supercell in configuration space. The additional translational symmetry of Eq. (10) may further reduce the irreducible portion of configuration space. If functions other than Bloch wave functions are used, then the irreducible portion of configuration space could be larger and more Monte Carlo sampling might be required to obtain accurate results.

In our DMC calculations we choose the initial configurations from the distribution $(\Phi^*_{\mathbf{k}_s,\mathbf{k}_p}\Phi_{\mathbf{k}_s,\mathbf{k}_p})$, where the guiding wave function $\Phi_{\mathbf{k}_s,\mathbf{k}_p}$ is obtained from a VMC calculation. States with different values of $\mathbf{k}_s$ or $\mathbf{k}_p$ are orthogonal and, therefore, the imaginary time propagation asymptotically generates the distribution $(\Psi^*_{\mathbf{k}_s,\mathbf{k}_p}\Phi_{\mathbf{k}_s,\mathbf{k}_p})$, where $\Psi_{\mathbf{k}_s,\mathbf{k}_p}$ is the best (lowest energy) wave function with wave vectors $\mathbf{k}_s$ and $\mathbf{k}_p$, which has the same nodal surface as $\Phi_{\mathbf{k}_s,\mathbf{k}_p}$ The DMC energy is calculated from

$$E_{\mathrm{DMC}} = \frac{\int (\Psi^*_{\mathbf{k}_s,\mathbf{k}_p}\Phi_{\mathbf{k}_s,\mathbf{k}_p})(\Phi^{-1}_{\mathbf{k}_s,\mathbf{k}_p}\hat{H}\Phi_{\mathbf{k}_s,\mathbf{k}_p})}{\int (\Psi^*_{\mathbf{k}_s,\mathbf{k}_p}\Phi_{\mathbf{k}_s,\mathbf{k}_p}).} \qquad (17)$$

E_{DMC} is real, but for arbitrary $\mathbf{k}_s$ and $\mathbf{k}_p$ vectors, the distribution $(\Psi^*_{\mathbf{k}_s,\mathbf{k}_p}\Phi_{\mathbf{k}_s,\mathbf{k}_p})$ is complex. We have not attempted to generate this distribution by a modified algorithm, such as the fixed-phase approximation of Ref. 19, but instead we have used the standard DMC algorithm for cases where both $\Psi_{\mathbf{k}_s,\mathbf{k}_p}$ and $\Phi_{\mathbf{k}_s,\mathbf{k}_p}$ can be chosen to be real. The fixed-node approximation[3,4] was implemented by rejecting any moves in which a node crossing was attempted. As is the case for the VMC calculations described earlier, all of the supercells in configuration space give equal contributions to Eq. (17), and the integrals need be performed only over a single supercell. In fact, we do not restrict the electron coordinates to be within a single supercell because this offers no computational advantage. However, if one wished to impose such a restriction, one would shift the electron coordinates into the chosen supercell by removing vectors in $\{\mathbf{R}_s\}$, which would multiply the wave function by a phase factor and may involve moving to a new nodal cell. Obviously such an arbitrary move to a new nodal cell must not be regarded as an attempt to cross the nodal surface.

The nodal cells of real many fermion wave functions always fall in to one or more classes, with nodal cells in the same class related by permutation symmetry.[20] Generating these classes is, in principle, straightforward. One chooses any electron configuration $\mathbf{R} = \{\mathbf{r}_1, \mathbf{r}_2, \ldots, \mathbf{r}_N\}$ at which the wave function, $\Psi(\mathbf{R})$, is nonzero. Application of all $N!$ permutation operators (including the identity) to $\mathbf{R}$ generates the set of points related to $\mathbf{R}$ by permutation symmetry. These $N!$ points lie in $N!$ or fewer different nodal cells, which make up the first class. If the cells in this class do not cover the configuration space, then a new class may be generated in the same way, starting with an arbitrary point lying in an unfilled nodal cell. Eventually, the configuration space will be covered, and all nodal cells will have been assigned to one of the different classes.

The tiling theorem[20] states that if $\Psi(\mathbf{R})$ is the ground state eigenfunction of a system of identical fermions, then all its nodal cells are in the same class. The theorem holds only for real ground states, but all eigenfunctions can be chosen to be real if the Hamiltonian has time reversal symmetry. Real eigenfunctions are not usually Bloch functions of the form of Eqs. (8) and (10), but are instead linear combinations of degenerate states with different wave vectors $\mathbf{k}_s$ and $\mathbf{k}_p$.

The proof of the tiling theorem is straightforward.

Suppose that the theorem is not true and that the ground state wave function $\Psi(\mathbf{R})$ contains two or more different classes of nodal cell. Construct a trial wave function by reversing the sign of Ψ within all nodal cells belonging to the mth class. This trial function is totally antisymmetric and has the same energy expectation value as $\Psi(\mathbf{R})$. Hence, it must also be a good ground state wave function, or a linear combination of degenerate ground states. This is impossible, however, since the trial function has slope discontinuities across the nodal surfaces joining cells of class m to cells of other classes, and so cannot even be an eigenfunction, never mind the ground state. We conclude that the initial hypothesis that Ψ was the ground state must have been wrong, and that the true ground state has only one class of nodal cell.

In a typical DMC calculation the nodal surface is imposed by using a guiding function, whose nodal surface is that of an LDA ground state wave function. The nodal surface of the guiding function is that of the ground state of a many-fermion problem (the noninteracting LDA problem) and so the tiling theorem applies. This does not mean that the nodal surface is exact — the nodes of the real interacting system may be quite different — but simply that all the nodal cells are related by permutation symmetry. It follows that DMC calculations in different nodal cells all give the same energy, and so a simulation in a single arbitrarily chosen cell is adequate in principle. In practice, we start with configurations generated from a VMC run and do not use this fact; but it does ensure that the final DMC energy is independent of the initial distribution of configurations.

The tiling theorem is not of great practical importance since the fixed-node DMC method gives a variational estimate of the ground state energy even when a guiding function with more than one class of nodal cell is used. However, DMC calculations in nodal cells belonging to different classes are not equivalent, and the *best* variational result consistent with the given nodal surface is obtained only if some of the configurations start out in nodal cells of the lowest energy class.

It is simple to extend the tiling theorem to show that all the nodal cells of the lowest energy wave function of a given $\mathbf{k}_s$ are related by symmetry, provided that the wave function can be chosen to be real. As mentioned previously, one can construct Bloch wave functions of the form of Eq. (8) which are real by choosing $\mathbf{k}_s = \mathbf{G}_s/2$, so that the states at $+\mathbf{k}_s$ and $-\mathbf{k}_s$ differ by the supercell reciprocal lattice vector $\mathbf{G}_s$, and are therefore equivalent. (Of course one can also generate real wave functions by choosing $\mathbf{k}_p = \mathbf{G}_p/2$.)

The extension of the tiling theorem relies on the fact that the irreducible representations of the translation group are one dimensional, so that there is a unique lowest energy wave function with a given $\mathbf{k}_s$. If this function can be chosen to be real then it can at most change sign when a single electron is translated by a supercell lattice vector. The nodal surface must, therefore, be invariant under such translations. The nodal cells of the lowest energy $\mathbf{k}_s$ wave function can be divided into classes just as before, except that now we use both permutations and translations in generating the members of a class. If the lowest energy state has more than one class of nodal cell, then again we can find a trial function of the same energy by reversing the sign in all nodal cells of one of the classes. This trial function is antisymmetric and has the same value of $\mathbf{k}_s$, but has cusps and so is not an eigenfunction. The lowest energy $\mathbf{k}_s$ eigenfunction cannot be degenerate with a function of the same $\mathbf{k}_s$, which is not even an eigenstate, and hence must have only one class of nodal cell.

VI. CALCULATIONS FOR GERMANIUM IN THE DIAMOND STRUCTURE

To illustrate the method of performing VMC and DMC calculations described above, we have performed a set of calculations for germanium in the diamond structure. In a previous paper,[11] we gave the results of similar calculations at the experimental equilibrium lattice constant of germanium of $a_0 = 5.65$ Å, while in this paper, we give results for the energy at seven different volumes. The single-particle orbitals from which the determinant for the trial or guiding wave function of Eq. (13) was constructed were obtained from self-consistent LDA calculations, and the Ge^{4+} ions were represented using a local pseudopotential of Starkloff-Joannopoulos form,[21]

$$V_{\rm ps}(r) = -\frac{Z}{r}\frac{(1-e^{-ar})}{(1+e^{a(r_c-r)})}, \qquad (18)$$

with $Z = 4$, $a = 18$, and $r_c = 1.05$. This pseudopotential has quite a hard core and to represent the LDA orbitals for the solid calculations we used a plane-wave basis set containing all waves up to a kinetic energy cutoff of 40 Ry. The local pseudopotential of Eq. (18) is significantly inferior to a fully norm-conserving nonlocal pseudopotential,[22] but tests using the LDA show that it is of similar quality to the best pseudo-Hamiltonian[23] that we could produce for Ge^{4+}.

We now discuss our choice of the states used to form the determinantal part of the trial/guiding wave function [Eq. (13)]. As mentioned in Sec. IV, we choose $\mathbf{k}_s = \mathbf{G}_s/2$, so that the mesh of $\mathbf{k}$ points in the primitive cell has inversion symmetry, which ensures that, for a closed shell configuration, a set of real orbitals can be formed. For our calculations we have used a fcc supercell, and in this case, there are three possible choices of $\mathbf{G}_s/2$ which lie within or on the surface of the supercell BZ: $\mathbf{G}_s/2 = (0,0,0)2\pi/a_s$, (where a_s is the cubic lattice constant of the supercell), $\mathbf{G}_s/2 = (1/2,1/2,1/2)2\pi/a_s$, and $\mathbf{G}_s/2 = (1,0,0)2\pi/a_s$, i.e., the Γ, L, and X points of the supercell BZ. In order to determine which of these vectors gives the best result, we performed a set of LDA calculations for supercells of sizes $1\times1\times1$ up to $8\times8\times8$, using each of these three choices of $\mathbf{k}_s$, and also a set of calculations, using $\mathbf{k}_s = \mathbf{k}_B = (0.6223, 0.2953, 0)2\pi/a_s$, where $\mathbf{k}_B$ is the Baldereschi mean-value point[13] of the supercell BZ. The calculated LDA energies per atom are plotted as functions of supercell size in Fig. 1, from which we can see that the energy from the Γ-*point* calculations converges quite slowly with increasing supercell

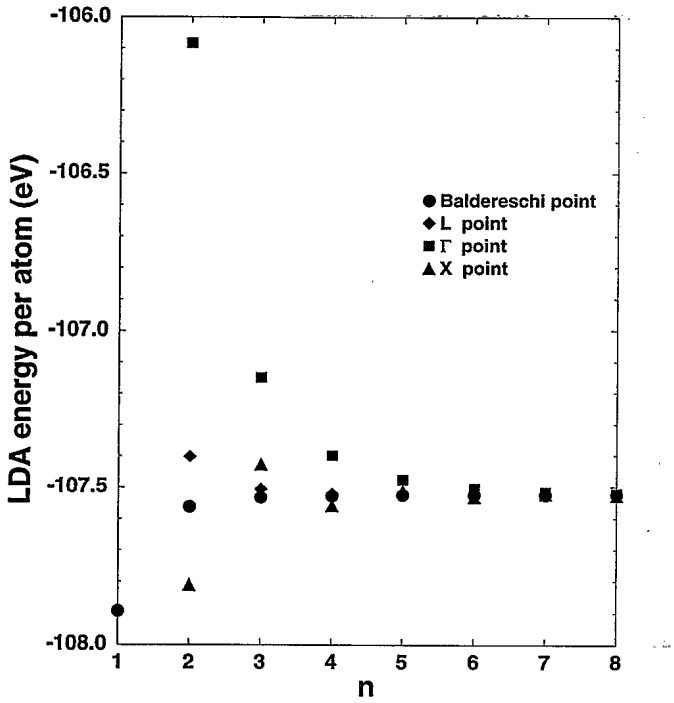

FIG. 1. Local-density approximation energies for $n \times n \times n$ supercells of diamond-structure germanium in eV per atom. $\mathbf{k}_s = (0,0,0)2\pi/a_s$ wave functions (squares), (where a_s is the cubic lattice constant of the supercell), $\mathbf{k}_s = (1/2,1/2,1/2)2\pi/a_s$ wave functions (diamonds), $\mathbf{k}_s = (1,0,0)2\pi/a_s$ wave functions (triangles), and $\mathbf{k}_s = \mathbf{k}_B = (0.6223,0.2953,0)2\pi/a_s$ wave functions (circles), where $\mathbf{k}_B$ is the Baldereschi mean-value point (Ref. 13) of the supercell BZ.

size, whereas the convergence of the X-point calculations is significantly better, and the L-point convergence is better still, and is only slightly inferior to the convergence of the Baldereschi point calculations. We have, therefore, chosen the L-point wave function for our QMC calculations. In fact, it turns out that if n_1, n_2, and n_3 are even, then this choice corresponds exactly to a MP mesh as defined in Ref. 14, while if any of n_1, n_2, or n_3 are odd, then a BZ integration performed with this mesh is superior to one using the corresponding MP mesh.

In our previous work,[11] we reported results of calculations for diamond-structure germanium at the equilibrium volume, which were performed with the same techniques as used here. Here, we report calculations for diamond-structure germanium as a function of volume. We have used $2 \times 2 \times 2$ fcc supercells containing 64 electrons, and have performed LDA, VMC, and DMC calculations using the L-point wave functions described above, which have $\mathbf{k}_p = 0$ and $\mathbf{k}_s = (1/2,1/2,1/2)2\pi/a_s$. An excellent description of the VMC method can be found in Ref. 9, and we follow the methodology given there closely. We have used an optimized Ewald method[24] to perform the Coulomb sums, in which the split between the real- and reciprocal-space functions is optimized for rapid convergence. For the calculations described here, this method is roughly three times faster than the standard Ewald technique.[25] The plane-wave basis set used to represent the single-particle orbitals in our calculations is very large ($\sim$ 1300 plane waves at the equilibrium volume), and the most expensive part of the calculation is the evaluation of these orbitals at the electron positions. We move one electron at a time, and for the VMC calculations the average distance of each attempted move was adjusted so that the acceptance/rejection ratio was approximately 50%. In order to obtain accurate statistics for the VMC results, 30 000 moves of all the electrons were made.

For the DMC calculations, we used the same $2 \times 2 \times 2$ supercells and the same trial/guiding wave functions as in the VMC calculations. The DMC calculations were performed using the fixed-node and short-time approximations. We used a time step of 0.015 a.u., which is the same value as used in the study of silicon by Li *et al.*,[10] who demonstrated that the resultant time-step error was small in that case. The average number of configurations in the ensemble was 200, and for each configuration 3000 moves of all the electrons were performed, except for the equilibrium volume where 5000 moves were performed.

The calculated LDA, VMC, and DMC energies are shown in Fig. 2(a). A number of corrections should be added to these results before proper comparisons can be made. The LDA energies shown in Fig. 2(a) were calculated using a 40 Ry basis set energy cutoff, and calculations performed with various cutoffs up to 125 Ry indicate that the infinite-basis-set LDA energies are approximately 0.12 eV per atom lower, essentially independent of volume. The VMC energies are expected to be lowered by a similar amount, but the DMC results are expected to be insensitive to the basis set used for the guiding wave function, as shown in Ref. 10. We also add finite-size corrections, which are of two types: (i) LDA finite-size corrections, and (ii) Coulomb finite-size corrections. The LDA finite-size correction is defined as the difference between the LDA result for a given supercell and the LDA result for a very large supercell (at the same energy cutoff of 40 Ry). The existence of a Coulomb finite-size effect, which is not included in the LDA, has been demonstrated by a number of previous calculations.[4,7,26] The need for such a correction can be seen by considering the case of jellium calculations using a supercell technique. In this case, the charge density is uniform whatever the supercell size, and, therefore, the LDA gives the same electron-electron interaction energy independent of supercell size. However, in a true many-body calculation with explicit electron-electron interactions, the interaction term in Eq. (1) is certainly a function of the supercell size, and, therefore, we expect an extra finite-size effect which is not included in the LDA, and is expected to be proportional to $1/r_s$, where r_s is the average density parameter.

The LDA and Coulomb finite-size corrections are approximated by

$$E^{\infty}_{\mathrm{QMC}} = E^{N}_{\mathrm{QMC}} + E^{\infty}_{\mathrm{LDA}} - E^{N}_{\mathrm{LDA}} + \frac{\alpha}{N r_s}, \qquad (19)$$

where E^{N}_{QMC} is the energy calculated using a QMC technique (VMC or DMC) for a supercell containing N electrons, E^{N}_{LDA} is the LDA energy for N electrons, and α is a

constant. The Coulomb correction term in Eq. (19) gives a volume dependent contribution to the QMC energies, because of the assumed $1/r_s$ dependence. The data given in Table I of our earlier paper[11] for $2\times2\times2$ and $3\times3\times3$ supercells of diamond-structure germanium at the experimental equilibrium lattice constant, which corresponds to $r_s = 2.086$, gives enough information to obtain values of the parameter α in several different ways. The Γ-point wave functions give $\alpha = 2.09$ a.u. (VMC data) and $\alpha = 1.88$ a.u. (DMC data), while the L-point wave functions give corresponding values of $\alpha = 2.16$ a.u. and $\alpha = 2.72$ a.u. To correct the L-point results reported here we have used $\alpha = 2.72$ a.u., which gives a Coulomb correction of +0.55 eV per atom for the $2\times2\times2$ supercell at the equilibrium volume. This Coulomb correction was not included in the results given in our earlier paper,[11] but in all other respects, the results for the equilibrium volume reported here are the same as in that paper. The Coulomb correction should not be added to the LDA results. At the equilibrium volume the LDA energy for the infinite supercell is −107.526 eV per atom (using a 40 Ry basis set cutoff), which gives a LDA finite-size correction of −0.12 eV per atom for the $2\times2\times2$ supercells used here. This correction is constant to within 0.015 eV per atom over the range of volumes considered, and we have neglected this small volume dependence. We found that within the LDA, and for very dense **k** point sampling the system was metallic at the volumes of 1.225 V_0, 1.15 V_0, and 0.775 V_0 but the effect on the energy was extremely small. For the finite supercells used in the QMC calculations there was no band overlap at any of the **k** points in the uniform mesh at any of the volumes.

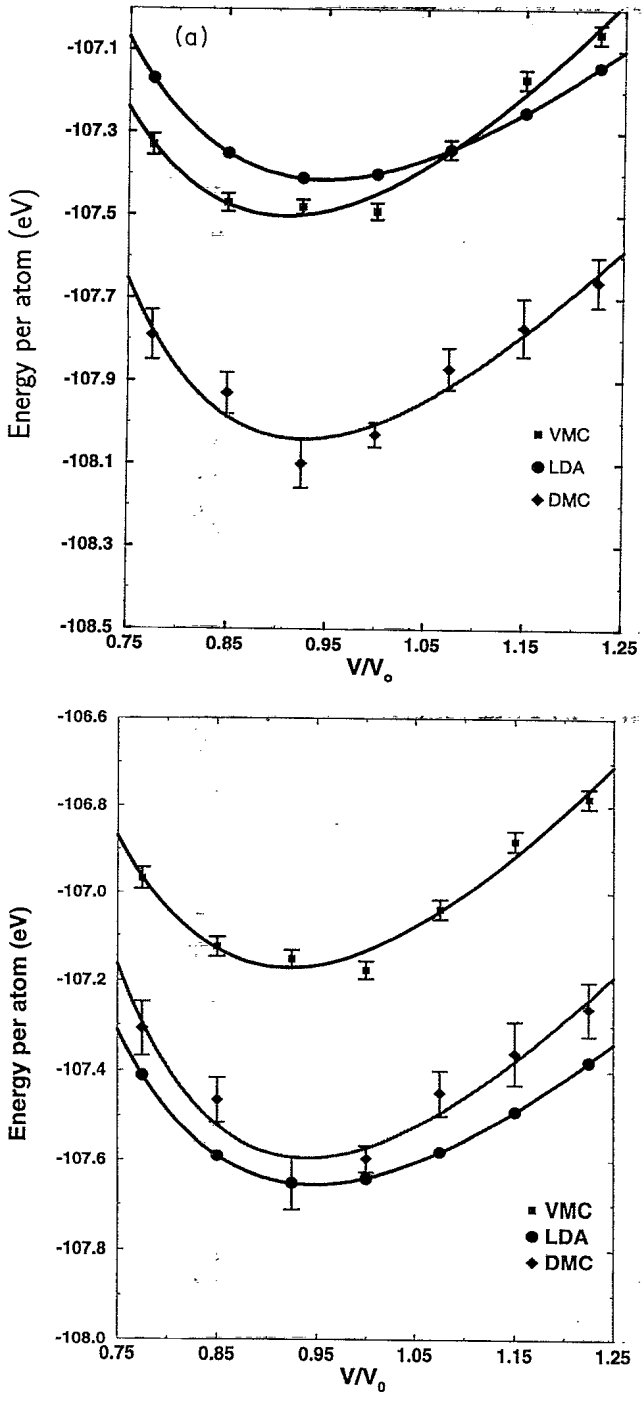

FIG. 2. (a) Uncorrected LDA (circles), VMC (squares), and DMC (diamonds) energies of diamond-structure germanium in eV per atom as functions of volume expressed as a fraction of the equilibrium volume of $V_0 = 22.55$ Å^3 per atom. The VMC and DMC energies are shown with error bars, which *indicate* single standard deviations. The continuous lines are guides to the eye.

TABLE I. Optimized values of the parameters α_n and β_n for the atomic $\chi(\mathbf{r})$ function of Eq. (20). The units are chosen so that the distances, r, in Eq. (20) must be given in atomic units.

	$n=0$	$n=1$	$n=2$	$n=3$
α_n	1.121 195	18.314 929	0.000 323	0.000 093
β_n	0.269 117	240.884 043	0.414 404	1.669 605

Including the basis set correction (LDA and VMC only), the LDA finite-size correction (LDA, VMC, and DMC) and the Coulomb finite-size correction (VMC and DMC only) to the original data of Fig. 2(a) gives our best estimates of the absolute energies for the LDA, VMC, and QMC methods, which are shown in Fig. 2(b). From Fig. 2(b) it is clear that our best estimate of the total energies, which are given by the corrected DMC results, are slightly higher in energy than the LDA results near the equilibrium volume. The results show a systematic trend in which, relative to the LDA energies, the VMC energies decrease as the volume is reduced. This effect is more pronounced in the data without corrections [Fig. 2(a)], but is still present in the corrected data. Unfortunately the statistical noise on the DMC data is too large to see whether the effect is present in this case. Earlier VMC and DMC results on silicon by Li *et al.*[10] using a pseudo-Hamiltonian approach[23] showed a similar effect in the VMC results, which was greatly reduced in the DMC data, from which they concluded that the trial wave function worked better at smaller volumes because the system was more uniform.

The statistical noise in the VMC and DMC data and the large volume range considered mean that it is not possible to obtain accurate values of the lattice constant and bulk modulus from the QMC data. These quantities

might be calculated using correlated sampling methods[27] which are especially suited for calculating energy differences between similar systems.

VII. ATOMIC CALCULATIONS

We have also performed VMC and DMC calculations for the germanium atom in the ^{3}P ground state configuration. For the VMC calculations, we used a single determinant wave function multiplied by a Jastrow factor and a one-body function, as in the solid calculations. The orbitals for the determinant were obtained from a non-spin-polarized spherically-symmetric LDA atomic calculation in the s^2p^2 configuration. We have also used orbitals obtained from a spin-polarized LSDA calculation, but the difference was negligible. For the Jastrow correlation factor, $u(r)$, we used the same form as in the solid calculations [Eq. (14)], with A=1.739767 a.u. and F_{σ_i,σ_j} chosen to satisfy the cusp conditions. Previous atomic calculations have often employed a Jastrow factor of the form $u(r) = -ar/(1+br)$, but in our experience this gives very similar results to Eq. (14).

The inclusion of the Jastrow factor certainly improves the description of correlation and so lowers the total energy, but it also acts to smooth out the charge density, giving a form greatly different from the accurate LDA charge density.[8,9] The charge smoothing effect of the Jastrow factor is more important in atoms than in solids, and is so severe for germanium that the Hartree-Fock and Hartree-Fock-Jastrow energies are very similar. The use of a one-body $\chi(\mathbf{r})$ function to counteract this charge smoothing is therefore essential. We have tested several forms for $\chi(\mathbf{r})$, limiting ourselves to spherically-symmetric functions, which were independent of the spin of the electrons, although of course for this atom the charge density is not spherically symmetric and the atom is spin polarized. First, we adopted the procedure of Fahy *et al.*[8,9] of constructing a $\chi(\mathbf{r})$ function, which brings the charge density towards the LDA form. Unfortunately, we found that the VMC energy was rather sensitive to the form chosen for $\chi(\mathbf{r})$ when fitting to the noisy data obtained from Eq. (15), and so this method was not very successful. A much better procedure is to assume no prior knowledge of the optimum electron density, but to determine $\chi(\mathbf{r})$ by minimizing the variance of the energy, which has been shown to be a successful technique for optimizing wave functions for QMC calculations.[28] We used a form for $\chi(\mathbf{r})$, consisting of a linear combination of even Hermite polynomials multiplied by Gaussians,

$$\chi(\mathbf{r}) = \sum_{n=o}^{3} \alpha_n H_{2n}(r) e^{-\beta_n^2 r^2} , \qquad (20)$$

where the parameters α_n and β_n were adjusted to minimize the variance of the VMC energy. The best value of the VMC energy obtained was −103.234(1) eV, using a four term expansion of $\chi(\mathbf{r})$. The optimized parameters α_n and β_n are given in Table I.

A DMC calculation for the germanium atom was performed using the optimized VMC wave function for the guiding function, giving an energy of −103.416(2) eV. The DMC energy for the atom is only 0.182 eV lower than the VMC energy, which indicates that the $u(r)$ function of Eq. (14) and the $\chi(\mathbf{r})$ function of Eq. (20), together with the LDA orbitals, gives a good approximation to the (fixed-node) wave function for the atom. For the solid, at the experimental volume, the DMC energy is 0.54 eV per atom lower than the VMC energy [see Fig. 2(a)], and, therefore, the solid wave function is not as accurate as the atomic one. This result illustrates one of the problems of VMC calculations; it is difficult to form wave functions of comparable accuracy for different systems. This problem is greatly alleviated in DMC calculations, although it is not altogether absent because the fixed node error will be different in the atom and solid.

The DMC atomic energy is 0.618 eV lower than the (spherically-symmetric and spin-polarized) LSDA result of −102.798 eV. This is similar to the difference of 0.85 eV obtained by Li *et al.*[10] for the silicon atom using a pseudo Hamiltonian. This result for silicon, and similar results for nitrogen,[12] have led the authors of Refs. 10 and 12 to conclude that the major error in the LSDA/LDA calculations is in the atomic energies, but we urge caution in this matter. As pointed out in Ref. 29, the (spherically-symmetric and spin-polarized) LSDA gives too large a magnitude of the sum of the four valence ionization energies of silicon and germanium, and, therefore, highly accurate calculations should give less binding than the LSDA for the four valence electrons, not more binding as has been found in QMC pseudopotential calculations. The resolution of this issue is not clear at the moment, but it may be that there is a significant transferability error when a pseudopotential created within a self-consistent field formalism is used in a QMC calculation. If this is correct then the QMC calculations could still give accurate cohesive energies because we would hope for a cancellation of this transferability error between the atom and solid calculations.

We now discuss the cohesive energy of germanium. The finite-size corrected DMC energy for the solid at the equilibrium volume is −107.60 eV per atom, as plotted in Fig. 2(b). Before we can compare with experiment, we must add two more corrections to this energy; a correction of +0.29 eV to account for the difference between the LDA cohesive energy calculated using a norm-conserving pseudopotential[29] and the value calculated with the local pseudopotential used here, and a correction of +0.04 eV from the zero-point motion. The DMC estimate of the cohesive energy is then 107.60 − 0.29 − 0.04 − 103.416 = 3.85 eV per atom, which is in fact precisely equal to the experimental value,[30] and is much better than the LDA result of 4.59 eV per atom.[29] The precise agreement with the experimental value should, of course, be viewed with caution. It is possible that the uncertainties in the DMC calculations could amount to an error of several tenths of an electron volt in the DMC cohesive energy, but we are confident that this error is much smaller than the error of 0.74 eV in the LDA cohesive energy. In our earlier work, we gave an estimate of the cohesive energy using

the $3 \times 3 \times 3$ supercell data of 4.01 eV,[11] and the difference between this value and our estimate of 3.85 eV is that our new estimate includes an additional Coulomb finite-size correction of 0.16 eV.

VIII. CONCLUSION

Many-body calculations for crystalline solids are normally carried out using a supercell which contains a number of primitive unit cells of the crystal. In this case, the Hamiltonian has two types of translational symmetry: (i) invariance under the translation of any electron coordinate by a supercell translation vector, and (ii) invariance under the translation of all electron coordinates by a translation vector of the underlying crystal lattice. These two symmetries lead to the existence of two wave vectors, which we denote as $\mathbf{k}_s$ and $\mathbf{k}_p$ [see Eqs. (8) and (10)], whose allowed values are linked by Eq. (12). Previous QMC calculations for the ground state properties of insulating solids have used wave functions with $\mathbf{k}_s = \mathbf{k}_p = 0$. We have shown that performing VMC and DMC calculations at nonzero values of $\mathbf{k}_s$ and/or $\mathbf{k}_p$ is straightforward. We have pointed out that the freedom to choose wave functions with different wave vectors allows the use of a set of ideas derived from band structure theory known as special k-points methods. For small supercells and insulating systems, these special k-points methods give results much closer to infinite-sized-supercell results than zero-wave vector calculations. A particularly advantageous choice is $\mathbf{k}_p = 0$ and $\mathbf{k}_s = \mathbf{G}_s/2$, where $\mathbf{G}_s$ is a supercell-reciprocal-lattice vector, which, for a closed shell configuration, allows the use of a real wave function. For the diamond-structure calculations reported here, we have used $\mathbf{k}_s = (1/2, 1/2, 1/2)2\pi/a_s$, which is closely related to a highly successful method of Brillouin zone integration introduced into band structure calculations by Monkhorst and Pack.[14] We have tested our methods by performing calculations on germanium in the diamond structure at seven different volumes, and find that using the special k-point methods reduces the finite-size effects considerably. The DMC energy for the germanium atom is considerably lower than the LSDA energy, while in the diamond-structure solid the DMC energy is slightly higher. The DMC value of the cohesive energy of germanium is very close to the experimental value, and is significantly smaller than the LSDA value.

ACKNOWLEDGMENTS

We thank M.Y. Chou, S. Fahy, B. Farid, and R. Haydock for helpful conversations, and the Engineering and Physical Sciences Research Council (U.K.) for financial support. The computations were performed on the Cray YMP-8 at the Rutherford-Appleton Laboratories (U.K.), and the Cray C-90 at the Pittsburgh Supercomputing Center (Grant No. DMR930039P).

[1] W.L. McMillan, Phys. Rev. **138**, A442 (1965); D. Ceperley, G.V. Chester, and M.H. Kalos, Phys. Rev. B **16**, 3081 (1977).
[2] D.M. Ceperley and M.H. Kalos, in *Monte Carlo Methods in Statistical Physics*, edited by K. Binder (Springer, Berlin, 1979); K.E. Schmidt and M.H. Kalos, in *Monte Carlo Methods in Statistical Physics II*, edited by K. Binder (Springer, Berlin, 1984); B.L. Hammond, W.A. Lester, and P.J. Reynolds, *Monte Carlo Methods in Ab Initio Quantum Chemistry* (World Scientific, Singapore, 1994).
[3] P.J. Reynolds, D.M. Ceperley, B.J. Alder, and W.A. Lester, J. Chem. Phys. **77**, 5593 (1982); D.M. Ceperley and B.J. Alder, *ibid.* **81**, 5833 (1984); R.M. Grimes, B.L. Hammond, P.J. Reynolds, and W.A. Lester, *ibid.* **85**, 4749 (1987).
[4] D.M. Ceperley, Phys. Rev. B **18**, 3126 (1978); D.M. Ceperley and B.J. Alder, Phys. Rev. Lett. **45**, 566 (1980).
[5] P. Ballone, C.J. Umrigar, and P. Delaly, Phys. Rev. B **45**, 6293 (1992).
[6] X.-P. Li, R.J. Needs, R.M. Martin, and D.M. Ceperley, Phys. Rev. B **45**, 6124 (1992).
[7] D.M. Ceperley and B.J. Alder, Phys. Rev. B **36**, 2092 (1987); V. Natoli, R.M. Martin, and D.M. Ceperley, Phys. Rev. Lett. **70**, 1952 (1993).
[8] S. Fahy, X.W. Wang, and S.G. Louie, Phys. Rev. Lett. **61**, 1631 (1988).
[9] S. Fahy, X.W. Wang, and S.G. Louie, Phys. Rev. B **42**, 3503 (1990).
[10] X.-P. Li, D.M. Ceperley, and R.M. Martin, Phys. Rev. B **44**, 10 929 (1991).
[11] G. Rajagopal, R.J. Needs, S. Kenny, W.M.C. Foulkes, and A. James, Phys. Rev. Lett. **73**, 1959 (1994).
[12] L. Mitas and R.M. Martin, Phys. Rev. Lett. **72**, 2438 (1994).
[13] A. Baldereschi, Phys. Rev. B **7**, 5212 (1973).
[14] H.J. Monkhorst and J.D. Pack, Phys. Rev. B **13**, 5188 (1976).
[15] W.R. Fehlner and S.H. Vosko, Can. J. Phys. **55**, 2041 (1978); A.H. MacDonald, Phys. Rev. B **18**, 5897 (1978).
[16] We use Hartree atomic units ($\hbar = e = m_e = 4\pi\epsilon_0 = 1$) for all equations.
[17] T. Kato, Commun. Pure Appl. Math. **10**, 151 (1957).
[18] D. Bohm and D. Pines, Phys. Rev. **92**, 609 (1953).
[19] G. Ortiz, D.M. Ceperley, and R.M. Martin, Phys. Rev. Lett. **71**, 2777 (1993).
[20] D.M. Ceperley, J. Stat. Phys. **63**, 1237 (1991).
[21] Th. Starkloff and J.D. Joannopoulos, Phys. Rev. B **16**, 5212 (1977).
[22] D.R. Hamann, M. Schlüter, and C. Chiang, Phys. Rev. Lett. **43**, 1494 (1979).
[23] G. Bachelet, D.M. Ceperley, and M.G.B. Chiochetti, Phys. Rev. Lett. **62**, 2088 (1988); W.M.C. Foulkes and M. Schlüter, Phys. Rev. B **42**, 11 505 (1990).
[24] G. Rajagopal and R.J. Needs, J. Comput. Phys. **115**, 399 (1994); V. Natoli and D.M. Ceperley, *ibid.* (to be published).
[25] P.P. Ewald, Ann. Phys. (Leipzig) **64**, 253 (1921); M.P. Tosi, Solid State Phys. **16**, 1 (1964), Appendix A.
[26] L. Fraser, W.M.C. Foulkes, G. Rajagopal, and R.J. Needs (unpublished).
[27] C.J. Umrigar, Int. J. Quantum Chem. **23**, 217 (1989).
[28] C.J. Umrigar, K.G. Wilson, and J.W. Wilkins, Phys. Rev. Lett. **60**, 1719 (1988).
[29] B. Farid and R.J. Needs, Phys. Rev. B **45**, 10 647 (1992).
[30] C. Kittel, *Introduction to Solid State Physics*, 6th ed. (Wiley, New York, 1986), p. 55, Table I. The data in this table were supplied by L. Brewer.